

Ordered equilibrium structures in soft matter systems between two and three dimensions

Mario Kahn,^a Jean-Jacques Weis,^b Christos N. Likos^c and Gerhard Kahl^{*a}

Received 6th April 2009, Accepted 22nd May 2009

First published as an Advance Article on the web 16th June 2009

DOI: 10.1039/b906832e

We identify the sequences of emerging ordered equilibrium structures as a three-dimensional crystal grows in thickness, starting from a two-dimensional lattice. To this end, we consider a system of particles that interact *via* a Gaussian potential and are confined between two parallel plates separated by a distance D . Using optimization tools that are based on genetic algorithms, we identify the $T = 0$, ground state configurations of the system. Based on these results, we investigate and interpret in detail two archetypes of structural transitions occurring in the diagram of states: one of them is a sequence of square \rightarrow centered rectangular \rightarrow hexagonal transitions at fixed confinement D as the density grows and the other is the often-discussed buckling transition, which emerges at fixed density as the system forms a new layer with increasing thickness D . These theoretical investigations are complemented and confirmed by Monte Carlo simulations.

The process of the gradual emergence of a three-dimensional crystal out of a two-dimensional lattice is highly intricate. The complexity of the sequences of structures as the crystal grows in thickness is an impressive demonstration of how nature optimizes, at every instant of the process, the positions of the particles under the condition that the energy of the arrangement is minimized. The first experimental investigations to elucidate this phenomenon were performed by Pieranski and co-workers, who studied the structure of polystyrene particles, confined in a wedge formed by two flat glass plates, giving thus rise to a progressively increasing layer thickness D .¹ Observed *via* an inverted metallurgical microscope, the authors of this remarkable study identified alternating sequences of square and triangular layered structures (to be denoted by \square and Δ , respectively). Experiments performed a few years later by Noser *et al.*,² revealed, in an essentially similar setup, a complex buckling mechanism, which emerges as a new layer is formed with increasing thickness D . The advent of new, experimentally refined techniques has led to the identification of even more complex transitions and structures as the system passes from n_l to $n_l + 1$ layers: occurrence of buckling, rhombic, prism or so-called hcp-perpendicular phases has been reported, as well as the identification of the complex S1 and S2 phases (see ref. 3 and references therein).

A first theoretical interpretation of the experimental results found by Pieranski *et al.*¹ was presented shortly thereafter by the same group,⁴ in which the particles were assumed to interact *via* a pure hard sphere potential. A few years later, a purely theoretical investigation was published,⁵ in which Chou and Nelson studied the structural phase transitions induced by the formation of a double layer out of a single layer within Landau theory, identifying, for the first time, a buckling transition. These theoretical predictions were compared in later studies with results obtained *via* density functional theory.⁶ However, most of the theoretical investigations on this phenomenon are based on simulations;^{7–10} a few of them being complemented by simple theoretical models. Very recently, a beautiful analogy between buckled colloidal monolayers and the triangular-lattice Ising antiferromagnet has been established in the work of Shokef and Lubensky.¹¹

While all these investigations unanimously confirm the transition $n_l \square \rightarrow n_l \Delta$, the findings about the emerging structural sequences in the transition $n_l \Delta \rightarrow (n_l + 1) \square$ are not consistent (*cf.* Table I of ref. 10). The reasons for these discrepancies are obvious: first – and this applies both to the experimental and theoretical investigations – these transitions occur in very narrow D -ranges (see discussion below), rendering an unambiguous identification of the emerging structures extremely difficult. Second, in experiments, which most commonly use a wedge geometry, a particular ordered phase at some given thickness D ‘grows out’ of a neighbouring ordered phase at a slightly smaller wall-distance and might therefore be strongly influenced by the latter. Thus, an entirely independent formation of an equilibrium structure at some given thickness D might be difficult to observe. Third, in computer simulations, an accurate identification of the complex transitional structures might be affected by the minute

Table 1 Reduced lattice sum $U/(N\epsilon)$ as a function of D for different competing ordered structures (as labelled by the symbols) for the buckling transition $n_l = 2 \rightarrow n_l = 3$ investigated at $\rho\sigma^3 = 0.1$. Close to the buckling transition, the respective lowest energy value is underlined

D/σ	$U/(N\epsilon)$		
	Δ ($n_l = 2$)	\mathcal{R} ($n_l = 6$)	\square ($n_l = 3$)
2.90	1.0674		
3.00		1.3582	
3.10		1.6335	
3.20		1.8916	
3.25		2.0092	
3.28		<u>2.0750</u>	2.0901
3.29		2.0960	<u>2.0910</u>
3.30			<u>2.0917</u>

^aCenter for Computational Materials Science (CMS) and Institut für Theoretische Physik, Technische Universität Wien, Wiedner Hauptstraße 8-10, A-1040 Wien, Austria

^bLaboratoire de Physique Théorique, UMR8627, Université Paris-Sud, F-91405 Orsay, France

^cInstitute for Theoretical Physics, Heinrich-Heine-Universität Düsseldorf, Universitätsstraße 1, D-40225 Düsseldorf, Germany

energy differences of the competing structures; in addition, a fixed shape of the simulation box entails the risk of suppressing or influencing the formation of particular structures. Finally, purely theoretical considerations are biased by the underlying, approximate concepts.

In this contribution, we report about an entirely different access to provide a deeper understanding of this complex process. Since the laws of statistical mechanics impose that the particles will arrange at given system parameters in such a way that the related thermodynamic potential is minimized, the search for the ordered equilibrium structure reduces to the minimization of this potential with respect to the lattice parameters. In an effort to solve this optimization task, we have applied search strategies that are based on genetic algorithms (GAs). In many applications in atomic or soft matter systems GAs were found to be highly reliable and efficient tools in identifying ordered equilibrium structures: they search basically the entire parameter space and cope extremely well with rugged energy landscapes in high-dimensional search spaces.^{12–14} In our access we restrict ourselves to $T = 0$ and investigate the formation of ordered structures for each D -value independently, avoiding thus several of the problems mentioned above. As a consequence of the vanishing temperature, the thermodynamic potential, which is in our case the free energy, reduces to the lattice sum U ; for our particular choice of particle interaction (to be specified below), U can be evaluated to within machine precision. With these considerations in mind and taking into account the extremely high success rate of GAs, we are able to present the ground state configurations for this system. Complementary computer simulations fully confirm a few assumptions that we had to make for computational reasons on the structure of the system.

In our system the particles are assumed to interact *via* a Gaussian potential, *i.e.*,

$$\Phi(r) = \varepsilon \exp[-(r/\sigma)^2] \quad (1)$$

where ε and σ represent energy- and length-scales; furthermore we introduce the (volume) number-density ρ . From the physical point of view the decision for the Gaussian core model (GCM) is motivated by the fact that this potential can be considered as a realistic coarse-grained, effective model for several colloidal dispersions, such as polymers,¹⁵ dendrimers,^{16,17} or microgels.¹⁸ In addition, there are also numerical reasons for our choice which we put forward in the following: (i) the *full* phase diagram of the GCM in three dimensions is known with high accuracy.^{19,20} Relevant for the present work is the fact that at very low temperatures the system solidifies for $\rho\sigma^3 \lesssim 0.1794$ in an fcc lattice, while for $0.1798 \lesssim \rho\sigma^3$ a bcc solid phase is predicted; (ii) since $\Phi(r) > 0$ for all r -values, there is no risk of compensation errors in evaluating the lattice sum, *i.e.*, the quantity that plays *the* key role in our search for ordered equilibrium structures. By extending the cut-off radius in the summation, r_{cut} , to a suitably large value, these sums can be evaluated for our model with arbitrary numerical precision.

We consider our system to be built up by n_l layers. The first assumption, (A1), is that the particles are not allowed to populate the space between the layers, they arrange within these layers in ordered, two-dimensional structures. Furthermore, we assume that these layers are arranged perpendicular to the z -axis, with the top and the bottom layers being fixed in their positions at $z = 0$ and $z = D$, respectively. Thus, we do not consider any particular wall–particle

interaction but restrict ourselves to pure confinement. The remaining $(n_l - 2)$ layers are allowed to arrange in vertical positions z_i with $0 \leq z_i \leq D$. Introducing $h_i = z_{i+1} - z_i$ (with $i = 1, \dots, n_l - 1$) as the vertical distance between layers i and $i + 1$, the restriction $\sum h_i = D$ has to be met. We point out that collapsing layers (*i.e.*, vanishing values for the h_i) are allowed within the formalism. The transition from the quasi-two- to the three-dimensional structure is realized by considering the limiting case $D \rightarrow \infty$.

For the population of the layers and for the ordered particle arrangements within the layers we make the two additional assumptions: (A2) the area number-density is the same in all layers and (A3) ordered structures in different layers are identical. While for the theoretical part of the study the above three assumptions represent a computational necessity, they will be fully confirmed by complementary computer simulations.

Within this model, the ordered structures of the system are characterized by stackings of two-dimensional lattices, specified by lattice vectors \mathbf{a} and \mathbf{b} , which form a simple unit cell. Furthermore, we introduce interlayer vectors \mathbf{c}_i , connecting the origins of layers i and $i + 1$; obviously, the z -component of \mathbf{c}_i is given by h_i . Non-simple, two-dimensional lattices are explicitly not considered in our parametrization, since any non-simple lattice (with n_b basis particles) can be realized by superposing n_b layers of vanishing vertical separation with identical, simple, two-dimensional structures. In total we are left with $(3n_l - 2)$ yet unknown quantities that have to be optimized.

These structural parameters are determined in a GA-based optimization search. To this end, a suitable code has been developed that is partly based on previous, successful GA-implementations for soft matter problems in two-^{21–23} and three-^{12,24–27} dimensional systems. Particular care has been dedicated to identify the two-dimensional lattice as uniquely as possible.²⁸ The quantity to be optimized is the free energy which reduces at vanishing temperature to the lattice sum, U . In evaluating this quantity, the potential was truncated at r_{cut} , which was typically chosen to be $\sim 4.3\sigma$: for this choice, $\int_{r_{\text{cut}}}^{\infty} \Phi(r) dr \lesssim \delta \int_0^{\infty} \Phi(r) dr$ with $\delta = 10^{-8}$. For the fitness function $f(\mathcal{S})$, which evaluates the quality of a candidate structure \mathcal{S} , we have chosen the canonical form¹², *i.e.*,

$$f(\mathcal{S}) = \exp[1 - U(\mathcal{S})/U(\mathcal{S}_0)] \quad (2)$$

where $U(\mathcal{S}_0)$ is the lattice sum of a reference square structure of the same density.

The computer simulations are standard NVT Monte Carlo (MC) simulations performed at $T^* = T/(k_B\varepsilon) = 0.002$, k_B being the Boltzmann constant. This temperature is sufficiently low to allow for a comparison with the theoretical results and guarantees that the system solidifies, apart from the very low density region (*i.e.*, $\rho\sigma^3 \leq 0.05$), in the entire density range.^{19,20} Similar to the theoretical considerations, the bottom and the top layers are fixed at $z = 0$ and $z = D$. In order to avoid any *a priori* restrictions on the emerging structures, the simulation cell was adaptive in the x - and y -directions.²⁹ Geometries with up to five layers were simulated, considering at least ~ 500 particles per layer. Simulations were extended over $2\text{--}6 \times 10^6$ trial moves per particle. In an effort to avoid any bias, different initial conditions for the MC runs were assumed. For most state points considered in the simulations we used the following strategy: for those states where, according to theoretical prediction, a rectangular structure is expected we started from a hexagonal

particle arrangement on pre-defined layers that are equally spaced between the confining walls, and *vice versa*. In addition, for selected state points MC runs were performed starting from more general initial configurations: either a random positioning of the particles on layers that are, again, equally spaced between $z = 0$ and $z = D$, or a completely random particle arrangement between the confining walls. The reason for these more general initial conditions was to check the validity of the assumptions (A1)–(A3) made for the parametrization of our model for the theoretical investigations (see above).

The GA-based, theoretical diagram of states is depicted in Fig. 1: on the one hand, it displays, by means of color-coding, the ordered equilibrium structures identified for each state point in a representative part of the (D, ρ) -plane. On the other, it provides information about the number of emerging layers, n_l : state points where the system consists of n_l layers form stripe-shaped regions that are separated by broken lines. These lines, which should for the moment only be considered as guides for the eye, represent the buckling transition which will be discussed below in detail. Apart from a region at low densities and small D -values where a rectangular double-layer structure is observed,³⁰ the diagram of states gives evidence that only three different ordered lattices occur: the hexagonal, the centered rectangular (to be denoted by \mathcal{R}), and the square structures. These particle arrangements populate the above mentioned stripe-shaped regions in a similar manner: in the lower part of each of these stripes we encounter square lattices which transform with increasing D and/or ρ via a centered rectangular lattice into a hexagonal lattice. Thus within a stripe-shaped region, these structures populate sub-stripes,³¹ which, with increasing n_l change in both shape and extent: while the hexagonal lattice populates, in all cases, a substantial portion of a stripe-shaped region, the area where the square-lattice is stable progressively reduces with increasing n_l at the cost of a growing stability range of the centered rectangular structure. The minute differences in energy of the competing structures make it impossible to decide whether for $n_l \geq 7$ the emergence of the square lattice is completely suppressed or whether this structure exists only in an extremely narrow range in parameter space.

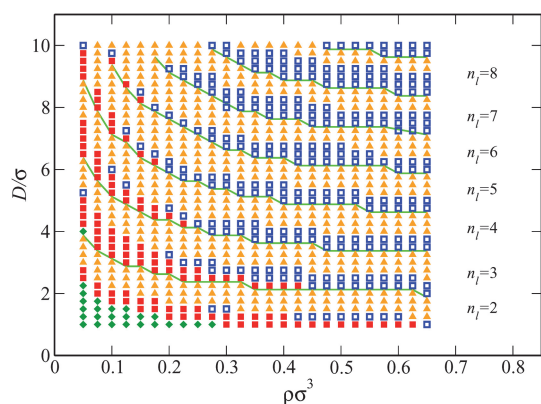


Fig. 1 Diagram of states for the layered system considered in this study, indicating the ordered structures assumed by the system at given values of thickness D and reduced density $\rho\sigma^3$: \blacklozenge = rectangular lattice, \blacksquare = square lattice, \blacktriangle = hexagonal lattice, and \blacksquare = centered rectangular. Regions where the system is composed of n_l layers are labeled by the respective n_l -value; these regions are separated by full lines.

The diagram of states was extracted from detailed GA-runs as follows: at fixed density ρ and layer number, n_l , optimizations have been performed over a representative D -range. The results of one of these GA-runs are depicted in Fig. 2 for $\rho\sigma^3 = 0.1$, where the (reduced) lattice sum, $U/(N\epsilon)$, N being the number of particles, is displayed as a function of D for different values of n_l : at some given D -value, the equilibrium structure is the one with the lowest value of the lattice sum U . The fact that, for instance, the U -curves coincide for $D \lesssim 3\sigma$ for $n_l = 2, 4$, and 6 indicates the internal consistency of our investigations: it reflects that a simple lattice ($n_l = 2$) can also be viewed as a non-simple lattice ($n_l = 4, 6$), formed by collapsing, horizontally shifted layers.

A closer inspection of the diagram of states reveals that all encountered structural transitions can essentially be reduced to two archetypes, which will be discussed in detail in the following. The first transition is the one occurring at fixed layer number, n_l , keeping the thickness D constant and varying ρ , or *vice versa*: it is the structural sequence $n_l\Box \rightarrow n_l\mathcal{R} \rightarrow n_l\Delta$. Obvious geometric considerations give evidence that this transition is continuous: considering all three structures (*i.e.*, \Box , \mathcal{R} , and Δ) as realizations of a centered rectangular lattice with a suitably chosen side-ratio, s , this transformation corresponds to a smooth variation of s from $s = 1$ (\Box) to $s = \sqrt{3}$ (Δ), as confirmed by the GA-based calculations. This change is nicely reflected in our simulation results when considering the orientational order parameters Ψ_4 and Ψ_6 (see, *e.g.*, ref. 32): this structural transition is reflected in a change in Ψ_6 from ~ 0 (\Box) to ~ 1 (Δ), and vice versa for Ψ_4 .

The second archetype of transition is the buckling transition, where the system creates, at fixed density and with increasing D (or *vice versa*), a new layer. With respect to the diagram of states (*cf.* Fig. 1) this means this transition pattern occurs whenever a line is crossed. From the numerical point of view these transitions are more difficult to observe, in particular for larger n_l -values and/or higher densities, where the identified intermediate structures occur in much smaller intervals of the parameters D and/or ρ . For the following discussion we have chosen the transition ($n_l = 2$) \rightarrow ($n_l = 3$) at fixed $\rho\sigma^3 = 0.1$, which we have identified to be the most

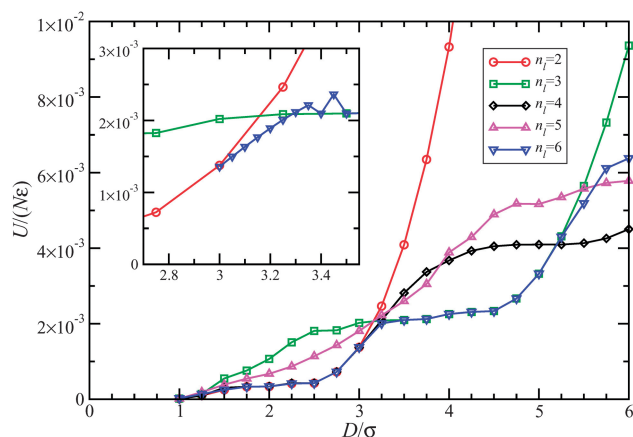


Fig. 2 Reduced dimensionless lattice sum $U/(N\epsilon)$ as a function of D at fixed density $\rho\sigma^3 = 0.1$ as obtained by GA-based optimization runs, considering different numbers of layers n_l as labeled. The inset displays the range $2.7 \leq D/\sigma \leq 3.5$ where the buckling transition from $n_l = 2$ to $n_l = 3$ occurs; for clarity only the results for $n_l = 2, 3$ and 6 are displayed.

pronounced manifestation of the buckling phenomenon. From the magnified view in Fig. 2, we see that for D -values up to $\sim 2.9\sigma$ a two-layer arrangement is the energetically most favourable one. On the structural level the situation is depicted in Fig. 3: particles form a hexagonal lattice in each of the two layers, *i.e.*, a structure that we can alternatively view as a centered rectangular lattice. We note that each of the two layers can be considered to be three collapsing, horizontally shifted sub-layers. By increasing D beyond 2.9σ , the two-layer structure transforms smoothly into a structure formed of six layers. This transition can be explained as follows: in the top and the bottom layers we now observe rectangular lattices formed by two of the aforementioned sub-layers; concomitantly, the particles of the third sub-layer that were formerly located in the centers of the rectangles rearrange in two additional layers that progressively detach from the bottom and the top layers; one might view these particles as tips of pyramids that have a rectangular basis in the top or in the bottom layers. By further increasing D , the rectangles reduce in size and the pyramids grow in height. At $D \sim 3.28\sigma$ this process comes to a sudden end. An increase in D now leads to a discontinuous transition: all of a sudden, the two inner layers merge, forming the newly created third layer; concomitantly, particles in the top and bottom layer spontaneously rearrange, forming square lattices. We mention that, despite considerable effort, we could not confirm the emergence of complex structures, such as those reported in experiment (see ref. 3 and references therein). Probably, these discrepancies are due to the fact

that the buckling transition occurs in very narrow D - and ρ -ranges and that competing structures are characterized by minute energy differences (*cf.* Table I). Thus, even tiny external perturbations in the experiment (see discussion above) can lead to metastable structures that do not correspond to the energetic minimum.

Our complementary MC simulations fully confirm the three assumptions on the parametrization of our theoretical model of the system. Starting from configurations where particles are randomly distributed in the simulation box, we observe that they tend to arrange in layers, leaving the inter-layer region essentially void; a more detailed discussion of these results will be discussed elsewhere. In the following we present results for the structures as obtained in MC simulations for the state point at $D = 4\sigma$ and $\rho\sigma^3 = 3.5$; as an initial condition we placed the particles on square lattices on predefined, equally-spaced layers. The snapshot in Fig. 4 gives qualitative evidence that the theoretical predictions of a centered rectangular structure are nicely confirmed in simulations. A more quantitative conclusion can be drawn from the pair distribution functions displayed in Fig. 5: nearest-neighbour distances as predicted by the theory are in excellent agreement with the peak positions in the pair distribution function extracted from the simulation. In addition, these results confirm the theoretical assumption that structures in the different layers are identical. Additional simulation data on the formation of ordered layer structures in general and on the buckling transition in particular will be published in due course.

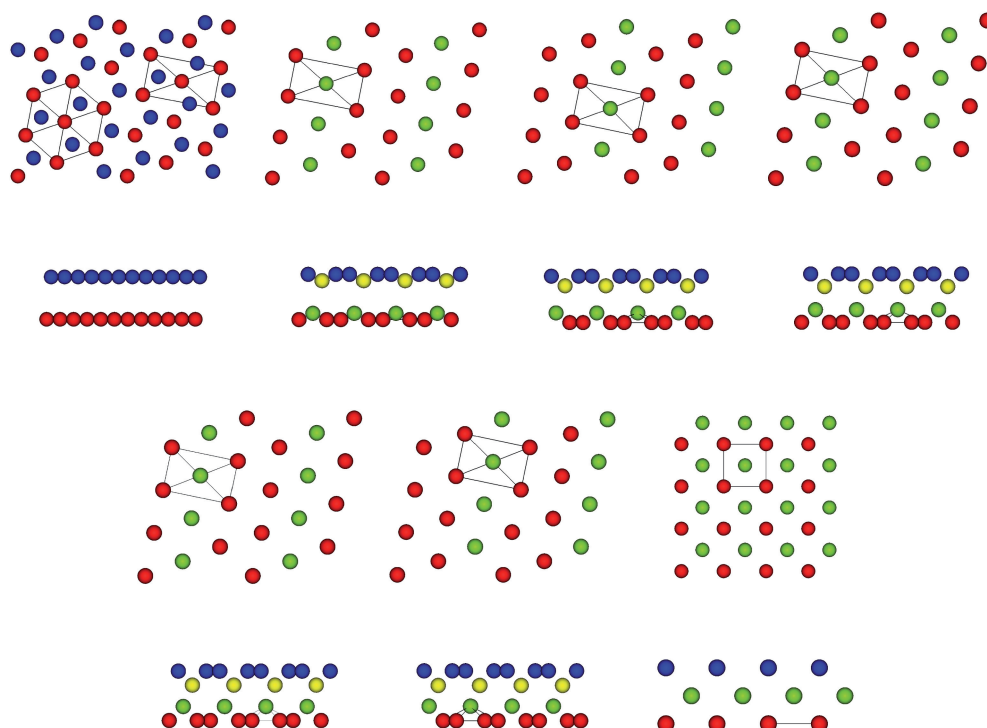


Fig. 3 Representation of the particle arrangement of an ordered equilibrium structure at density $\rho\sigma^3 = 0.1$ as the system transforms from a two- to a three-layer structure (buckling transition). The D -values considered are $D/\sigma = 2.9, 3.0, 3.1, 3.2, 3.25, 3.28,$ and 3.29 , from left to right and top to bottom. Displayed are the top and the side views of the ordered structures, where in the former case in general only the lower-half of the ordered structure is displayed; in the upper-half an identical, but shifted particle arrangement is found. In addition, unit cells that characterize the underlying structure are marked as guides for the eye (see also text).

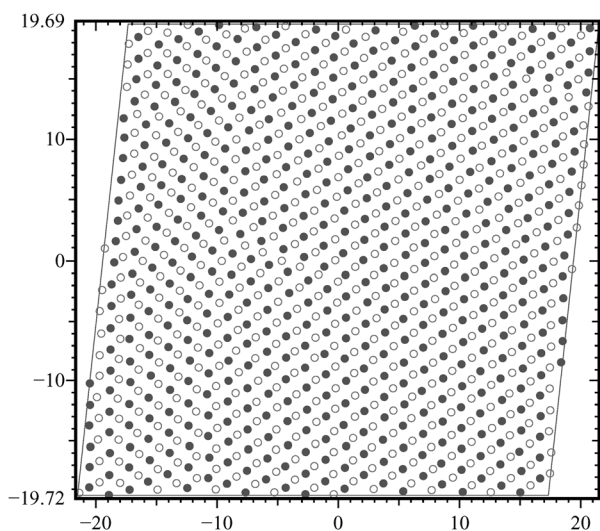


Fig. 4 Simulation snapshot of a layered system at $D = 4\sigma$ and $\rho\sigma^3 = 0.35$; only the particle positions in the two lower layers (specified by the different shading) are displayed. 529 particles per layer have been considered. The initial simulation box was quadratic with a side length of 40σ ; its shape at the instant of the snapshot is delimited by the thin grey lines. Extensions of the simulation box in x - and y -directions are given in units of σ .

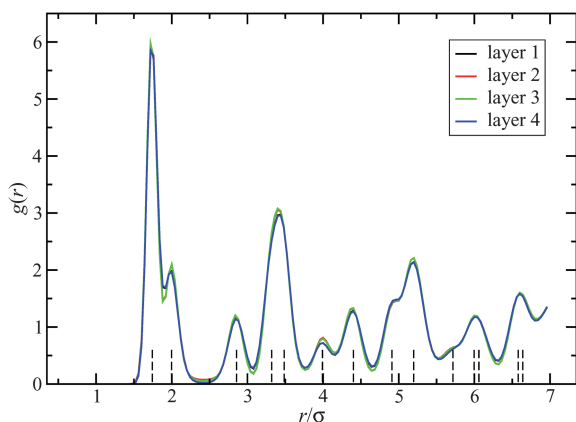


Fig. 5 Pair distribution functions $g(r)$ for the layered system for $D = 4\sigma$ and $\rho\sigma^3 = 0.35$ as functions of r , evaluated separately for the four different layers in computer simulations. Vertical bars indicate distances between particles in the corresponding ordered structure as predicted by theory; the height of these bars is proportional to the number of neighbours at this distance.

Using GA-based optimization techniques and complementary MC simulations we have investigated the ordered equilibrium structures that emerge as a three-dimensional lattice grows in thickness D . Using a Gaussian-shaped interparticle potential we are able to discern between energetically competing ordered equilibrium particle arrangements at given D and number-density ρ with high accuracy. Two archetypes of transition scenarios have been identified from the diagram of states. We give evidence that in particular the buckling

transition occurs in a very narrow energy interval, thus providing an impressive demonstration of the system's efforts to arrange particles at every instant in such a way that the energy of the system is optimized. We point out that a finite temperature (and thus the entropic contributions to the thermodynamic potential) will certainly have an impact on the layered structures. Using the bulk behavior of the Gauss model as a guidance,¹⁹ we can expect that the $T = 0$ phase transition boundaries between the ordered phases will not be drastically altered by the entropic contributions at finite temperature. However, at temperatures around $k_B T/\epsilon \cong 10^{-2}$, order is expected to be lost and the system should undergo a transition to a (confined) fluid phase, whose density profile will be inhomogeneous in the direction perpendicular to the walls and uniform parallel to the same. The solution of this computationally more demanding task will be the topic of future investigations.

We thank Dieter Gottwald and Julia Fornleitner (both Wien) as well as T. Palberg, A.B. Fontecha, and H.-J. Schöpe (all Mainz) for helpful discussions. This work was funded by the FWF, Proj. Nos17823-N08 and P19890-N16 and by the DFG within the SFB-TR6, Project Section C3. JJW and GK gratefully acknowledge financial support by the Programme Hubert Curien AMADEUS under Project Nos 13815TF and FR 09/2007.

Notes and references

- 1 P. Pieranski, L. Strzelecki and B. Pansu, *Phys. Rev. Lett.*, 1983, **50**, 900.
- 2 S. Naser, C. Bechinger, P. Leiderer and T. Palberg, *Phys. Rev. Lett.*, 1997, **79**, 2348.
- 3 A. B. Fontecha and H.-J. Schöpe, *Phys. Rev. E: Stat., Nonlinear, Soft Matter Phys.*, 2008, **77**, 061401.
- 4 B. Pansu, P. Pieranski and P. Pieranski, *J. Phys. (Paris)*, 1984, **45**, 331.
- 5 T. Chou and D. R. Nelson, *Phys. Rev. E: Stat., Nonlinear, Soft Matter Phys.*, 1993, **48**, 4611.
- 6 H. Bock, K. E. Gubbins and K. G. Ayappa, *J. Chem. Phys.*, 2005, **122**, 094709.
- 7 M. Schmidt and H. Löwen, *Phys. Rev. Lett.*, 1996, **76**, 4552.
- 8 M. Schmidt and H. Löwen, *Phys. Rev. E: Stat., Nonlinear, Soft Matter Phys.*, 1997, **55**, 7228.
- 9 R. Zangi and S. A. Rice, *Phys. Rev. E: Stat., Nonlinear, Soft Matter Phys.*, 2000, **61**, 660.
- 10 A. Fortini and M. Dijkstra, *J. Phys.: Condens. Matter*, 2006, **18**, L371.
- 11 Y. Shokef and T. C. Lubensky, *Phys. Rev. Lett.*, 2009, **102**, 048303.
- 12 D. Gottwald, G. Kahl and C. N. Likos, *J. Chem. Phys.*, 2005, **122**, 204503.
- 13 A. R. Oganov and C. W. Glass, *J. Phys.: Condens. Matter*, 2008, **20**, 064210.
- 14 S. M. Woodley and R. Catlow, *Nat. Mater.*, 2008, **7**, 937.
- 15 A. A. Louis, P. G. Bolhuis, J. P. Hansen and E. J. Meijer, *Phys. Rev. Lett.*, 2000, **85**, 2522.
- 16 C. N. Likos, S. Rosenfeldt, N. Dingenouts, M. Ballauff, P. Lindner, N. Werner and F. Vögtle, *J. Chem. Phys.*, 2002, **117**, 1869.
- 17 I. O. Götze, H. M. Harreis and C. N. Likos, *J. Chem. Phys.*, 2004, **120**, 7761.
- 18 A. R. Denton, *Phys. Rev. E: Stat., Nonlinear, Soft Matter Phys.*, 2003, **67**, 011804; A. R. Denton, Erratum, *Phys. Rev. E: Stat., Nonlinear, Soft Matter Phys.*, 2003, **68**, 049904.
- 19 A. Lang, C. N. Likos, M. Watzlawek and H. Löwen, *J. Phys.: Condens. Matter*, 2000, **12**, 5087.
- 20 S. Prestipino, F. Saija and P. V. Giaquinta, *Phys. Rev. E: Stat., Nonlinear, Soft Matter Phys.*, 2005, **71**, 050102.
- 21 J. Fornleitner and G. Kahl, *Europhys. Lett.*, 2008, **82**, 18001.
- 22 J. Fornleitner, F. Lo Verso, G. Kahl and C. N. Likos, *Soft Matter*, 2008, **4**, 480.
- 23 J. Fornleitner, F. Lo Verso, G. Kahl, and C. N. Likos, *Langmuir* (in press), DOI: 10.1021/1a900421v.

-
- 24 G. J. Pauschenwein and G. Kahl, *Soft Matter*, 2008, **4**, 1396.
- 25 G. J. Pauschenwein and G. Kahl, *J. Chem. Phys.*, 2008, **129**, 174107.
- 26 G. J. Pauschenwein and G. Kahl, *J. Phys. (Condens. Matter)* (in press).
- 27 T. Tückmantel, F. Lo Verso, and C. N. Likos, *Mol. Phys.* (in press).
- 28 M. Kahn, Diploma-thesis (TU Wien, 2008) unpublished.
- 29 D. Frenkel and B. Smit, *Understanding Molecular Simulation*, Academic Press, London, 2nd edn, 2002.
- 30 Note that similar structures are observed in dipolar colloidal systems confined in a quasi-planar geometry; cf. J. Fornleitner, PhD thesis, Technische Universität Wien, 2008, (unpublished).
- 31 The rugged contour of the different regions in the diagram of states is a consequence of the finite grid size that has been used for our investigations.
- 32 K. J. Strandburg, *Rev. Mod. Phys.*, 1988, **60**, 161.